2950 Niles Road, St. Joseph, MI 49085-9659, USA
269.429.0300 fax 269.429.3852 hq@asabe.org www.asabe.org

An ASABE Meeting Presentation
DOI: https://doi.org/10.13031/aim.202100901
Paper Number: 2100901

ANALYTICAL MODELING SOIL REACTION FORCES ON ROTARY TILLER

Bakhadir Mirzaev[1*], Brian Steward[2], Farmon Maмatov[3], Mehari Tekeste[2], Mansur Amonov[1]

[1] Tashkent Institute of Irrigation and Agricultural Mechanization Engineers, Tashkent, 100000, Uzbekistan
[2] Iowa State University, Ames, IA 50011, USA
[3] Karshi branch of Tashkent Institute of Irrigation and Agricultural Mechanization Engineers, Karshi, 180100, Uzbekistan

***Correspondence: bakhadir.mirzaev@bk.ru; bakhadir.mirzaev@tiiame.uz**

Written for presentation at the
2021 Annual International Meeting
ASABE Virtual and On Demand
July 12–16, 2021

ABSTRACT. Rotary tillers with flat tines are widely used in agriculture. In this study, the power requirement of an active tillage tool was investigated using a theoretical procedure. The goal of this work was to determine and analyze the soil resistance forces on the tine of rotary tiller. The laws and rules of theoretical mechanics were applied in the research. Theoretical studies obtained analytical relationships for determining the soil resistance forces acting on the chamfers and side surfaces of the tines of the rotary tiller, as well as the torques associated with these forces. The analysis of the obtained analytical expressions showed that the forces of the tiller tine is mainly influenced by the mode of operation of the tiller, the design parameters of the tine and the physical and mechanical properties of the soil. With an increase in the index of the kinematic mode of operation, λ, which is the ratio of the peripheral speed of the tine to the forward speed of the tiller, the resistance force of the flat tine decreases, and then takes a negative value. At $\lambda > 2$, the resistance force of the tine is directed towards direction of movement. In this case, a driving force is formed, the maximum value of which is reached at λ =2-2.2

Keywords. modeling, reaction force, rotary tiller, tine, soil properties

INTRODUCTION

Rotary tillers are widely used in agriculture. Rotary tilling has a positive effect on the physical properties of the soil, water and nutrient regimes of plants [1]. In addition, active rotary tillers are used as an additional working body on plows [2-4], deep-diggers and combined tillage machines [5-22]. Active working bodies such as rotary tillers of tillage machines, along with technological functions, will also perform the functions of movers and thus allows unloading a narrow link in the chain of energy transmission through the tractor's drive, and will also contribute to increasing the productivity and efficiency of the machine unit [2-6].

For loosening of compacted top soil layers and grinding plant residues, active rotary tillers with flat tines in combination with passive working bodies have been widely used [2-3]. Flat tines require low tillage energy and create crumbling of soil, because soil after tillage with rotary tiller is exposed to the passive working bodies of tillage machines. The flat tines of active rotary tiller can be installed radially, with the tine inclined from the radius to direction of rotation or backward [1]. When installing tines with a slope from the radius in the course of rotation, the pinching of the cut plant residues, so that does not consider the interaction of tines of this type of rotary tiller.

Researchers have modeled the soil-tool interaction of active tillage systems including both rotary harrows and and tillers. Most of the work has been associated with rotary tillers which generally use L-shaped blades rotating about a horizontal axis. Hendrick and Gill's seminal work [25-29] described the effect of rotary tiller design parameters on tillage operation. Thakur and Godwin [30] summarized the models of soil reaction forces on the tines of rotary tillers. More recent work has investigated effects of kinematic and kinetic models on specific work [23] and the size of soil slices of rotary tillers [24].

The purpose of study is to predict analytically the draft forces of an active rotary tiller with straight tines as the tools interact with soil.

METHODS AND MATERIALS

Mathematical modeling based on theoretical agricultural soil mechanics were applied to predict draft forces from rotary tiller with straight tines. In the process of operation, the active rotary tine overcomes the reactive soil resistance forces and soil frictional forces that have arisen at the soil-blade/chamfers systems from the soil to soil and soil to tine surfaces (Fig. 1). By decomposing the soil resistance forces to cutting and frictional into horizontal and vertical components from the schematics in figure-1, we obtain:

$$R_x = R_{bx} - F_{bx} + N_{fx} + T_x + F_x, \tag{1}$$

$$P_y = P_{by} - P_{by} + N_{fy} + T_y + F_y, \tag{2}$$

where:

R_{bx}, R_{by}, F_{bx} and F_{by} = horizontal and vertical components of the soil resistance and friction forces acting on the tine/knife blade;

N_{fx}, N_{fx}, T_x and T_y = horizontal and vertical components of the soil resistance and friction forces acting on the knife hamfers;

F_x and F_y = horizontal and vertical components of the soil resistance and friction forces that occur on the side surfaces of the knife/tine.

E.g.

R_{bx}, = horizontal soil resistance;

N_{fx}, N_{fx}, T_x and T_y = horizontal and vertical components of the soil resistance and friction forces acting on the tine/knife chamfers;

F_x and F_y = horizontal and vertical components of the soil resistance and friction forces that occur on the side surfaces of the knife/tine.

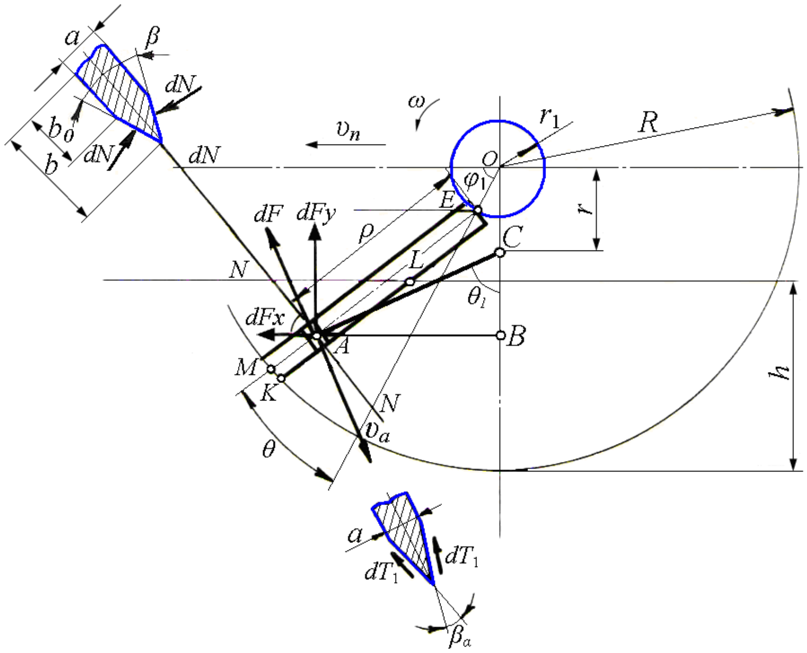

Figure 1. Scheme for determining the soil resistance forces acting on the chamfers and side surfaces of the tine/knife

When cutting soil and plant residues with a knife/tine, a force N_b, occurs on its blade, directed along the normal $N – N$ (Fig. 1 and 2).

$$N_b = \sigma_b \delta l_b, \tag{3}$$

where:
σ_b = breaking contact tension;
δ = blade thickness;
l_b = blade working length

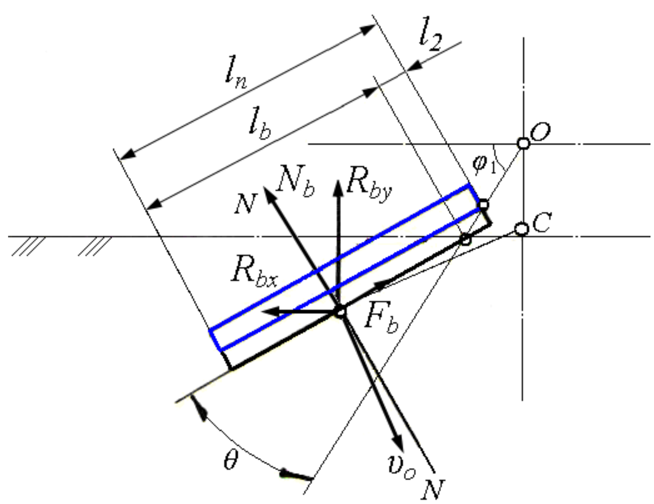

Figure 2. Scheme for determining the soil resistance forces acting on the knife/tine blade

From Fig. 1 we have

$$l_b = KL = l_n - \frac{2(R - hr_1 \sin\varphi_1) + b\cos(\varphi_1 + \theta)}{2\sin(\varphi_1 - \theta)}, \tag{4}$$

where
R = rotary tiller radius;
h = depth of soil loosening;
l_n = tine/knife length

Substituting of l_b value to expression (4) in (3) and decomposing the force N_b into horizontal and vertical components, we have

$$R_{bx} = \sigma_b \delta \left[l_n - \frac{2(R - h - r_1 \sin\varphi_1) + b\cos(\varphi_1 - \theta)}{2\sin(\varphi_1 - \theta)} \right] \cos(\varphi - \theta), \tag{5}$$

$$R_{by} = \sigma_b \delta \left[l_n - \frac{2(R - h - r_1 \sin\varphi_1) + b\cos(\varphi_1 - \theta)}{2\sin(\varphi_1 - \theta)} \right] \sin(\varphi_1 - \theta). \tag{6}$$

On the blade of the knife, there are frictional forces, the value of which depends on the value of the angle α between the normal *N-N* and the absolute velocity υ_a. When $\alpha \geq \varphi$ $F_b = fN_b = N_b tg\varphi$, and when $\alpha < \varphi$ $F_b = N_b tg\alpha$. At the same time, for the corresponding position of the knife at the specified λ, R, h, θ and r_1, it is necessary to determine the length of the blade l_α, on which $\alpha < \varphi$ and the length of the blade l_φ, on which $\alpha < \varphi$. After that, possible define the components F_x and F_y of total friction force $F^\wedge$.

For the part of the blade on which $\alpha \geq \varphi$:

$$F_{bx} = \sigma_b \delta l_\alpha tg\varphi \sin(\varphi_1 - \theta), \tag{7}$$

$$F_{by} = \sigma_b \delta l_\alpha tg\varphi cos(\varphi_1 - \theta). \tag{8}$$

For the part of the blade on which $\alpha < \varphi$:

$$F_{bx} = \sigma_b \delta l\varphi tg\alpha \sin(\varphi_1 - \theta), \tag{9}$$

$$F_{by} = \sigma_v \delta l\varphi tg\alpha cos(\varphi_1 - \theta). \tag{10}$$

Resultant of the normal soil pressures N_c acting on the tine/knife chamfers

$$N_c = 2N_{c1} \sin\beta = pal_b, \tag{11}$$

where
a = knife/tine thickness

By decomposing N_c into horizontal and vertical components we get:

$$N_{cx} = pa \left[l_n - \frac{2(R - h - r_1 \sin\varphi_1) + b\cos(\varphi_1 - \theta)}{2\sin(\varphi_1 - \theta)} \right] \cos(\varphi_1 - \theta), \tag{11, 12}$$

$$N_{cy} = pa \left[l_n - \frac{2(R - h - r_1 \sin\varphi_1) + b\cos(\varphi_1 - \theta)}{2\sin(\varphi_1 - \theta)} \right] \sin(\varphi_1 - \theta). \tag{12, 13}$$

From the normal force N_c on the chamfers of the tine/knife, friction forces T_{c1} arise. The elementary force dT_{c1} is directed in the direction opposite to the direction of the absolute velocity of the center point of the elementary chamfer site.

The projection of the friction forces dT_{c1} on the plane of the knife is equal to

$$dT = 2dT_1 \cos\beta_\alpha = fpa \frac{\cos\beta_\alpha}{\sin\beta_\alpha} d\rho. \tag{14}$$

Then

$$dT_x = fpactg\beta_\alpha \cos\theta_1 d\rho, \tag{15}$$

$$dT_y = fpactg\beta_\alpha \sin\theta_1 d\rho, \tag{16}$$

where
β_α = the angle of the knife sharpening in the plane deviated from the normal plane to the cutting edge of the knife by the angle α. To simplify the calculations, we accept $\beta_\alpha = \beta$.

From the triangle *ABC* (Fig. 1) we have

$$\cos\theta_1 = \frac{BC}{AC}, \qquad \sin\theta_1 = \frac{AB}{AC},$$

$$BC = \rho\sin(\varphi_1 - \theta) + r, \sin\varphi_1 - r_1, \tag{17}$$

$$AB = \rho\cos(\varphi_1 - \theta) + r, \cos\varphi_1 - r_1, \tag{18}$$

$$AC = \sqrt{\rho^2 + 2\rho\left[r_1\cos(\varphi_1 - \theta)\cos\varphi + \sin(\varphi_1 - \theta)(r_1 - \sin\varphi_1 - r)\right] + r_1^2 - 2rr_1, \sin\varphi_1 + r^2}, \tag{19}$$

where

r = the distance from the axis of rotation of the knife to the instantaneous center of rotation, that is, to the point C.

Denoting

$$m = r_1\cos(\varphi_1 - \theta)\cos\varphi_1 + (r_1\sin\varphi_1 - r)\sin(\varphi_1 - \theta), \tag{20}$$

$$n = r_1^2 - 2rr, \sin\varphi_1 + r^2 \tag{21}$$

we have

$$AC = \sqrt{\rho_2 + 2\rho m + n}\,. \tag{22}$$

Then

$$T_x = fpactg\beta \int_{l_1}^{l_n} \frac{\rho\sin(\varphi_1 - \theta) + r_1\sin\varphi_1 - r_1}{\rho^2 + 2\rho m + n} d\rho, \tag{23}$$

$$T_y = fpactg\beta \int_{l_1}^{l_n} \frac{\rho\cos(\varphi_1 - \theta) + r_1\cos\varphi_1 - r_1}{\rho^2 + 2\rho m + n} d\rho \tag{24}$$

Calculating the integrals obtained, we get

$$T_x = fpactg\beta\left\{\sin(\varphi_1 - \theta)(A_2 - A_1) + \left[r_1\sin\varphi_1 - r - m\sin(\varphi_1 - \theta)\right]\ln\left(\frac{l_n + m + A_2}{l_1 + m + A_1}\right)\right\}, \tag{13, 25}$$

$$T_y = fpactg\beta\left\{\cos(\varphi_1 - \theta)(A_2 - A_1) + \left[r_1\cos\varphi_1 - r - m\cos(\varphi_1 - \theta)\right]\ln\left(\frac{l_n + m + A_2}{l_1 + m + A_1}\right)\right\}, \tag{14, 26}$$

where

$$A_1 = \sqrt{\rho_2 + 2m\rho_1 + n}\,, \quad A_2 = \sqrt{\rho_2 + 2m\rho_1 + n}\,. \tag{27}$$

By selecting the elementary site dS on the surface of the knife we determine the components of the elementary reactions of the soil from the forces of friction and adhesion

$$dF = 2fPdS = 2fPb_0 d\rho,$$

$$dF_x = 2fPb_0\cos\theta_1 d\rho, \tag{15, 28}$$

$$dF_y = 2fPb_0\sin\theta_1 d\rho, \tag{16, 29}$$

where

b_0 = knife base width

From fig. 1 we have

$$b_o = \frac{2btg\beta - a}{2tg\beta}. \tag{30}$$

By inserting the values $\cos\theta_1$ and $\sin\theta_1$ to (28) and (29) we get

$$F_x = 2fpb_0 \int_{l_2}^{l_n} \frac{\rho \sin(\varphi_1 - \theta) + r_1 \sin\varphi_1 - r_1}{\sqrt{\rho^2 + 2\rho m + n}} d\rho, \tag{31}$$

$$F_y = 2fpb_0 \int_{l_2}^{l_n} \frac{\rho \cos(\varphi_1 - \theta) + r_1 \cos\varphi_1 - r_1}{\sqrt{\rho^2 + 2\rho m + n}} d\rho, \tag{32}$$

$$l_2 = l_n - \frac{R - h - r\sin\varphi_1}{\sin(\varphi_1 - \theta)}. \tag{33}$$

After calculating the obtained integral expressions, we will have

$$F_x = 2fpb_0 \left\{ \sin(\varphi_1 - \theta)(A_2 - A_1) + \left[r_1 \sin\varphi_1 - r - m\sin(\varphi_1 - \theta) \right] \ln\left(\frac{l_n + m + A_2}{l_2 + m + A_1}\right) \right\}, \tag{17, 34}$$

$$F_y = 2fpb_0 \left\{ \cos(\varphi_1 - \theta)(A_2 - A_1) + \left[r_1 \cos\varphi_1 - r - m\cos(\varphi_1 - \theta) \right] \ln\left(\frac{l_n + m + A_2}{l_2 + m + A_1}\right) \right\}. \tag{18, 35}$$

The obtained analytical expressions allow us to determine the components of the soil resistance forces acting on the rotary tiller tine/knife under different operating modes, depending on the design parameters of the tine/knife and the physical and mechanical properties of the soil.

The torque M_c supplied to the rotary tiller from the tractor power take-off shaft is spent on overcoming the moments from the reactive resistance forces and soil friction forces acting on the blade, chamfers and side surfaces of the tine/knife, that is

$$M_c = M_R + M_{Fb} + M_n + M_T + M_F, \tag{36}$$

where
M_R and M_{Fb} = moments from the soil's resistance and friction forces acting on the tine/knife blade;
M_n and M_T = moments from the resistance and friction forces acting on the chamfers of the tine/knife;
M_E = moments from the friction forces acting on the side surfaces

From fig. 3 we have

$$dM_R = dR_b h_b = \sigma_b \delta h_b d\rho, \tag{37}$$

$$dM_N = dN_{cb} h_b = pah_b d\rho, \tag{38}$$

where

$$h_b = r_1 \cos\theta + \rho. \tag{39}$$

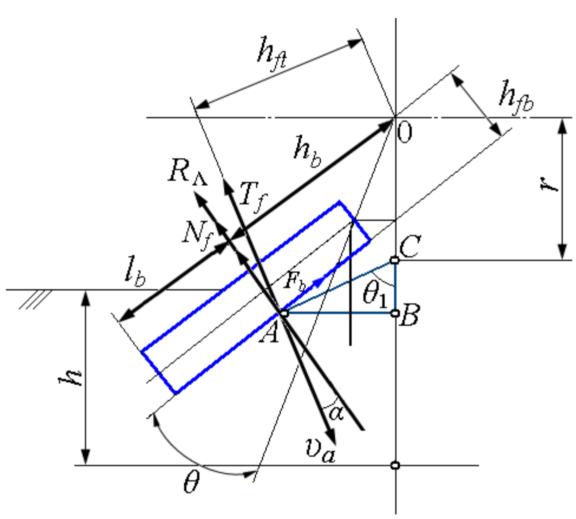

Figure 3. Scheme for determining the moments from the soil resistance forces acting on the cutter blade

Then

$$M_R = \int_{l_1}^{l_n} \sigma_b \delta (r_1 \cos\theta + \rho) d\rho, \tag{40}$$

$$M_N = \int_{l_1}^{l_n} pb(r_1 \cos\theta + \rho) d\rho. \tag{41}$$

After calculating the integral expressions, we get

$$M_R = \sigma_b \delta r_1 \left[\cos\theta (l_n - l_1) + (l_n - l_1)^2\right], \tag{19, 42}$$

$$M_N = pbr_1 \left[\cos\theta (l_n - l_1) + (l_n - l_1)^2\right]. \tag{20, 43}$$

The moment M_{Fb} of the soil friction force acting on the blade is determined by the following expression

$$M_{Fb} = F_b h_{fb} F_b (r_1 \sin\theta + \frac{b}{2}). \tag{21, 44}$$

The elementary friction forces dt and dF acting on the chamfers and the side surfaces of the tine/knife create elementary moments of resistance equal to

$$dM_T = dTh_T = fpactg\beta_{cp} h_T d\rho, \tag{22, 45}$$

$$dM_T = dTh_T = fpactg\beta_{cp} h_T d\rho. \tag{23, 46}$$

From the fig. 3 we have

$$h_T = AC + r\cos\theta \tag{47}$$

After substituting the values of AC and $\cos\theta$ to dependence (45) and (46), we will have:

$$M_T = fpactg\beta_{cp} \left[\int_{l_1}^{l_n} \sqrt{\rho^2 + 2m\rho + n} + \alpha\rho + r \int_{l_1}^{l_n} \frac{\rho \sin(\varphi_1 - \theta) + r_1 \sin\varphi_1 - r}{\sqrt{\rho^2 + 2m\rho + n}} d\rho \right], \tag{24,48}$$

$$M_F = 2fpb_0 \left[\int_{l_1}^{l_n} \sqrt{\rho^2 + 2m\rho + n} + \alpha\rho + r \int_{l_1}^{l_n} \frac{\rho \sin(\varphi_1 - \theta) + r_1 \sin\varphi_1 - r}{\sqrt{\rho^2 + 2m\rho + n}} d\rho \right]. \tag{49}$$

After calculating the obtained integral expressions, we have

$$M_T = fpactg\beta_{cp} \left\{ \begin{array}{l} \frac{l_n + m}{2} A_2 - \frac{l_1 + m}{2} A_1 + \frac{n - m_2}{2} \ln(\frac{l_n + m + A_2}{l_1 + m + A_1}) r\cos(\varphi_1 - \theta)(A_2 - A_1) + \\ + r[r\cos\varphi_1 - m\cos(\varphi_1 - \theta)] \ln(\frac{l_n + m + A_2}{l_1 + m + A_1}) \end{array} \right\}, \tag{25,50}$$

$$M_F = 2fpb_0 \left\{ \begin{array}{l} \frac{l_n + m}{2} A_2 - \frac{l_1 + m}{2} A_1 + \frac{n - m_2}{2} \ln(\frac{l_n + m + A_2}{l_1 + m + A_1}) r\cos(\varphi_1 - \theta)(A_2 - A_1) + \\ + r[r\cos\varphi_1 - m\cos(\varphi_1 - \theta)] \ln(\frac{l_n + m + A_2}{l_1 + m + A_1}) \end{array} \right\}. \tag{51}$$

The algebraic sum of expressions (42-44, 48, 50) will represent the resistance moment Ms of the tiller when tine/knife interacts with the soil. The obtained dependences allow us to analyze the nature of change in Ms depending on position of the tine/knife in the soil (φ_1), design parameters and operating modes of the tiller, as well as physical and mechanical properties of the soil.

The results of determining the physical, mechanical and technological properties of soils are presented. It is established that before plowing the fields have a pronounced uneven relief, characterized by the presence of ridges and irrigation furrows. The average height of the ridges in fields with row spacing of 90 and 60 cm is 17.1 and 12.8 cm, respectively. The physical, mechanical and technological properties of the soil of the arable and sub-arable layer of the cotton field along the wheel track differ significantly from the soil between the rows without the wheel track and the ridge: the density of the soil along the wheel track of the soil reaches 1.65 g / cm3, which is correspondingly greater than the density of the ridge soil by 0.24; the density, hardness and resistance of the soil to various deformations has a maximum value in the layers of 15-25 cm along the track of the tractor wheels.

Results and Discussion

In fig 4 and 5 are graphs of horizontal soil reaction dependence of the soil interacting with the tiller blade R_x on angle of rotation of tiller φ_1 and the kinematic parameter λ of the tiller at α =10 mm, b =65 mm, β =200, R =300 mm, r =100 mm, r =150 mm, l_n =210 mm, f=0.5, p =6010^{-4} Pa, σ_b =350 10^{-4} Pa, δ =100 microns, h =150 mm.

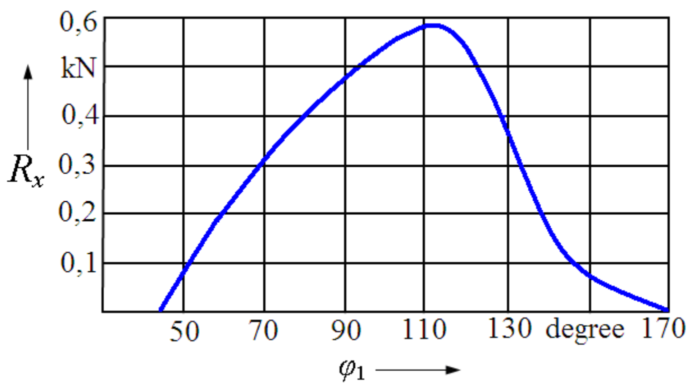

Figure 4. Change in the total soil horizontal reaction acting on the rotary tiller tine from the angle of rotation

From fig. 4, it can be seen that each rotary tiller tine at λ=2 creates a pushing force R_x =0.58 kN. The maximum pushing force is created at λ =2-2.2 (fig 5). A further increase in λ slightly increases the value of R_x. This reduces the total pushing force due to the movement of the adjacent tine/knife on the loosened soil. Thus, at λ =2-2. 2, the maximum pushing force is created, soil spraying is excluded, and the required energy for the rotary tiller drive is reduced.

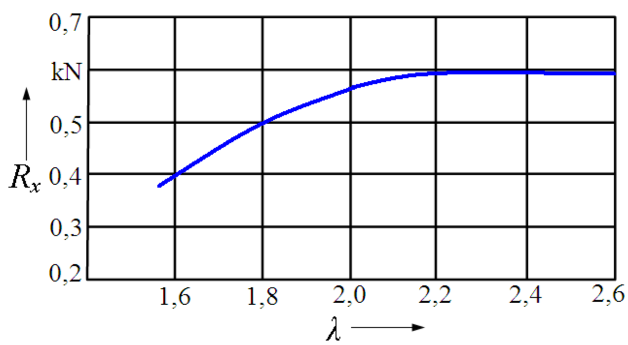

Figure 5. Determination total horizontal reaction of soil acting on rotary tiller tine from the kinematic mode of operation

Conclusions

From this research, the following conclusions can be drawn:

1. Analytical dependences for determining soil resistance forces acting on the blade, chamfers and side surfaces of knife/tine of active rotary tiller, as well as moments from these forces, were obtained. The analysis of obtained analytical expressions showed that main influence on traction resistance of tiller tine/knife is mode of operation of tiller, the design parameters of tine/knife and physical and mechanical properties of the soil.

2. It is established that the maximum pushing force of the rotary tiller tine/knife is created when kinematic mode of operation equal to λ=2,2-2,4.

3. The impact of the force from the rotary cultivator in the soil bin and field to verify the mathematical prediction

will be made in future researches

REFERENCES

[1] Sineokov G.N., Panov I.M. Teorija i raschet pochvoobrabatyvajushih mashin. – M.: Mashinostroenie, 1977. –328 s. [In Russian].

[2] Medvedev V.I. Energetika mashinnyh agregatov s rabochimi organami-dvizhiteljami. – Cheboksary: Chuvash. kn. izd-vo, 1972. [In Russian].

[3] Homenko M.S. i dr. Perspektivy ispol'zovanija pochvoobrabatyvajushih mashin s aktivnymi i passivnymi rabochimi organami // Mehanizacija i jelektrifikacija sel'skogo hozjajstva. – №5 –1987– s.26-28. [In Russian].

[4] Mamatov, F., Mirzaev, B., Mirzahodzhaev, Sh., Uzakov, Z and Choriyeva, D. Development of a front plow with active and passive working bodies // IPICSE 2020. IOP Conf. Series: Materials Science and Engineering 1030 (2021) 012164. IOP Publishing. doi:10.1088/1757-899X/1030/1/012164.

[5] Chatkin M.N. Sovremennye problemy zemledel'cheskoj mehaniki. Pahotnyj agregat s aktivnymi predpluzhnikami // Tehnika v sel'.hoz-ve. – 1990. -№ 4. – s. 33. [In Russian].

[6] Chatkin M.N., Kuprjashkin V.F. Osobennosti dinamicheskogo analiza raboty pochvoobrabatyvajushhih frezernyh agregatov /

Mehanizacija i jelektrifikacija sel. hoz-va. – 2006. -№ 12. – S.9-11. [In Russian].

[7] Aldoshin, N., Mamatov, F., Ismailov, I., Ergashov, G. Development of combined tillage tool for melon cultivation // 19th international scientific conference engineering for rural development Proceedings, Jelgava, 20.-22.05.2020. Volume 19. ISSN 1691-5976. DOI:10.22616/ERDev.2020.19.TF175.

[8] Umurzakov, U., Mirzaev, B., Maмatov, F., Ravshanov, H., Kurbonov, S. A rationale of broach-plow's parameters of the ridge-stepped ploughing of slopes // XII International Scientific Conference on Agricultural Machinery Industry IOP Conf. Series: Earth and Environmental Science 403(2019) 012163 IOP Publishing doi:10.1088/1755-1315/403/1/012163.

[9] Mirzaev, B., Mamatov, F., Chuyanov, D., Ravshanov, X., Shodmonov, G., Tavashov, R and Fayzullayev, X. Combined machine for preparing soil for cropping of melons and gourds // XII International Scientific Conference on Agricultural Machinery Industry. doi.org/10.1088/1755-1315/403/1/012158.

[10] Mirzaev, B., Mamatov, F., Ergashev, I., Ravshanov, H., Mirzaxodjaev, Sh., Kurbanov, Sh., Kodirov, U and Ergashev, G. Effect of fragmentation and pacing at spot ploughing on dry soils // E3S Web of Conferences 97. doi.org/10.1051/e3sconf/201913501065.

[11] Mirzaev, B., Mamatov, F., Aldoshin, N and Amonov, M. Anti-erosion two-stage tillage by ripper // Proceeding of 7th International Conference on Trends in Agricultural Engineering 17th-20th. September 2019 Prague, Czech Republic. – pp.391-396.

[12] Mamatov, F., Mirzaev, B., Tursunov, O. A Justification of Broach-Plow’s Parameters of the Ridge-Stepped Ploughing // E3S Web of Conferences 97, 05035 (2019). doi.org/10.1051/e3sconf/20199705035.

[13] Mamatov, F., Mirzaev, B., Tursunov, O., Ochilov, S and Chorieva, D. Relief, physico-mechanical and technological properties of soil in the cotton growing area // ICECAE 2020. IOP Conf. Series: Earth and Environmental Science 614(2020) 012169. IOP Publishing. doi:10.1088/1755-1315/614/1/012169.

[14] Umurzakov, U., Mamatov, F., Aldoshin, N., and Mirzaev, B. Exploration of tillage technologies in the Republic of Uzbekistan // ICECAE 2020 IOP Conf. Series: Earth and Environmental Science 614(2020) 012168. IOP Publishing. doi:10.1088/1755-1315/614/1/012168.

[15] Mamatov, F., Aldoshin, N., Mirzaev, B., Ravshanov, H., Kurbanov, Sh and Rashidov, N. Development of a frontal plow for smooth, furless plowing with cutoffs // IPICSE 2020. IOP Conf. Series: Materials Science and Engineering 1030 (2021) 012135 IOP Publishing. doi:10.1088/1757-899X/1030/1/012135.

[16] Mamatov, F., Ergashev, I., Mirzaev, B., Pardaev, X, Chorieva, D. Research of the Penetration Process of the Frontal Plow // 2nd Bukittinggi International Conference on Education (BICED) 2020. Journal of Physics: Conference Series 1779 (2021) 012002. IOP Publishing. doi:10.1088/1742-6596/1779/1/012002.

[17] Kodirov, U., Aldoshin, N., Ubaydullayev, Sh., Sharipov, E., Muqimov, Z and Tulaganov, B. The soil preparation machine for seeding potatoes on comb // CONMECHYDRO – 2020 IOP Conf. Series: Materials Science and Engineering 883(2020) 012143 IOP Publishing doi:10.1088/1757-899X/883/1/012143.

[18] Ravshanov, Kh., Fayzullaev, Kh., Ismoilov, I., Irgashev, D., Mamatov, S. The machine for the preparation of the soil in sowing of plow crops under film // CONMECHYDRO – 2020 IOP Conf. Series: Materials Science and Engineering 883(2020) 012138 IOP Publishing doi:10.1088/1757-899X/883/1/012138.

[19] Ravshanov, H, Babajanov, L, Kuziev, Sh, Rashidov, N, Kurbanov, Sh. Plough hitch parameters for smooth tails// CONMECHYDRO – 2020 IOP Conf. Series: Materials Science and Engineering 883(2020) 012139 IOP Publishing doi:10.1088/1757-899X/883/1/012139.

[20] Chuyanov, D., Shodmonov, G.,Avazov, I., Rashidov, N, Ochilov, S. Soil preparation machine parameters for the cultivation of cucurbitaceous crops // CONMECHYDRO – 2020 IOP Conf. Series: Materials Science and Engineering 883(2020) 012139 IOP Publishing doi:10.1088/1757-899X/883/1/012122.

[21] Ahmetov A.A. Sozdanie kombinirovannoj mashiny s rotacionnymi rabochimi organami dlja predposevnoj obrabotki pochvy na zasolennyh zemljah: Diss. …dokt. tehn. nauk. – Tashkent, 2015. – 75 s. [In Russian].

[22] Panov I.M. Vybor jenergosberegajushhih sposobov obrabotki pochvy // Traktory i sel'skohozjajstvennye mashiny. – №8 –1990– S.32-33.

[23] Ahmadi, I. (2017). A torque calculator for rotary tiller using the laws of classical mechanics. *Soil and Tillage Research*, *165*, 137-143.

[24] Celik, A., & Altikat, S. (2008). Geometrical analysis of the effects of rotary tiller blade path on the distribution of soil slice size. *Applied Engineering in agriculture*, *24*(4), 409-413.

[25] Hendrick, J. G., & Gill, W. R. (1971a). Rotary-Tiller Design Parameters Part I-Direction of Rotation. *Transactions of the ASAE*, *14*(4), 669-674, 683.

[26] Hendrick, J. G., & Gill, W. R. (1971b). Rotary tiller design parameters Part II-depth of tillage. *Transactions of the ASAE*, *14*(4), 675-678.

[27] Hendrick, J. G. and Gill, W. R. (1971c). Rotary tiller design parameters Part III – Ratio of peripheral and and forward velocities. *Transactions of the ASAE, 14*(4): 679-683.

[28] Hendrick, J. G., & Gill, W. R. (1974). Rotary Tiller Design Parameters Part IV-Blade Clearance Angle. *Transactions of the ASAE*, *17*(1), 4-7.

[29] Hendrick, J. G., & Gill, W. R. (1978). Rotary tiller design parameters, V: Kinematics. *Transactions of the ASAE*, *21*(4), 658-660.

[30] Thakur, T. C., & Godwin, R. J. (1989). The present state of force prediction models for rotary powered tillage tools. *Journal of Terramechanics*, *26*(2), 121-138.